

On Applying the Lackadaisical Quantum Walk Algorithm to Search for Multiple Solutions on Grids

Jonathan H. A. de Carvalho^{*1}, Luciano S. de Souza², Fernando M. de Paula Neto¹, and Tiago A. E. Ferreira²

¹Centro de Informática, Universidade Federal de Pernambuco, Recife, Pernambuco, Brasil
{jhac,fernando}@cin.ufpe.br

²Departamento de Estatística e Informática, Universidade Federal Rural de Pernambuco, Recife, Pernambuco, Brasil
{luciano.serafim,tiago.espinola}@ufrpe.br

Abstract

Quantum computing holds the promise of improving the information processing power to levels unreachable by classical computation. Quantum walks are heading the development of quantum algorithms for searching information on graphs more efficiently than their classical counterparts. A quantum-walk-based algorithm that is standing out in the literature is the lackadaisical quantum walk. The lackadaisical quantum walk is an algorithm developed to search two-dimensional grids whose vertices have a self-loop of weight l . In this paper, we address several issues related to the application of the lackadaisical quantum walk to successfully search for multiple solutions on grids. Firstly, we show that only one of the two stopping conditions found in the literature is suitable for simulations. We also demonstrate that the final success probability depends on the space density of solutions and the relative distance between solutions. Furthermore, this work generalizes the lackadaisical quantum walk to search for multiple solutions on grids of arbitrary dimensions. In addition, we propose an optimal adjustment of the self-loop weight l for such scenarios of arbitrary dimensions. It turns out the other fits of l found in the literature are particular cases. Finally, we observe a two-to-one relation between the steps of the lackadaisical quantum walk and the ones of Grover's algorithm, which requires modifications in the stopping condition. In conclusion, this work deals with practical issues one should consider when applying the lackadaisical quantum walk, besides expanding the technique to a wider range of search problems.

1 Introduction

Advantages came from using quantum phenomena — such as superposition, interference, and entanglement [1] — have been attracting significant research efforts to conceive quantum algorithms more efficient than their classical counterparts. The major milestone to be reached is the so-called quantum supremacy, which will demonstrate the superiority of quantum computing

^{*}Corresponding author

over classical computing [2]. Recently, Google claimed to have reached this quantum supremacy milestone [3]. However, IBM claimed to have refuted Google’s experiment by using advanced classical techniques [4]. Nonetheless, this episode represents remarkable advances in mastering the technology available in the current times of noisy intermediate-scale quantum hardware [5].

Even if practical quantum computers may not be available, quantum algorithms have already proven some speedup over classical analogues. One of the most known examples is the quantum algorithm proposed by Grover [6] for searching a disordered array. Grover’s algorithm can successfully search for a single element within a disordered database of N items in $O(\sqrt{N})$ steps, which is a quadratic speedup over the best known classical counterparts. However, if the task is a spatial search, Benioff [7] showed that a quantum robot using Grover’s algorithm is no more efficient than a classical robot because both require $O(N \log \sqrt{N})$ steps to search 2-dimensional grids of size $\sqrt{N} \times \sqrt{N}$. This makes room for employing other techniques to search information on physical grids modeled as connected graphs [8], also known as spatial search problems.

Quantum walk is a remarkably promising class of algorithms that already provided gains in practical problems [9, 10, 11, 12, 13], besides shown universal as a model for quantum computation [14, 15]. As classical random walks, the quantum walks are divided into discrete-time and continuous-time models, which were respectively introduced in [16] and [17]. However, these discrete-time and continuous-time models of quantum walks are not fundamentally equivalent because a model cannot be obtained from the other model by discretization or approaching time steps to zero [18]. Actually, Childs [19] obtained a continuous-time quantum walk as an appropriate limit of discrete-time quantum walks, although there are examples of Hamiltonians in which this correspondence between models fails.

Experimentally, researchers have been trying to find the most efficient model of quantum walks, mainly in spatial search problems, which is just the task where Grover’s algorithm failed to give speedup [7]. Firstly, Childs and Goldstone [20] addressed a 2D spatial search problem using a continuous-time quantum walk but failed to provide substantial speedup. After, Ambainis et al. [21] proposed an algorithm capable of finding the solution after $O(\sqrt{N} \log N)$ steps using a discrete-time model, outperforming the previous works. However, Childs and Goldstone [22] achieved this same runtime later using a continuous-time model.

Over time, quantum walks for other graph structures have been developed, such as for hypercubes and complete graphs [23, 24, 25], but attempts to improve the search on 2D grids continued as well. In particular, the lackadaisical quantum walk (LQW) developed in [26] has been drawing attention because it improved the 2D spatial search by making a simple modification to the algorithm proposed in [21]. The modification was to attach a self-loop of weight l at each vertex of the 2D grid. Adding a new degree of freedom to enable staying at the same position had already been studied for the quantum walk on the line [27]. The LQW, in turn, added a weighted edge that points to the same vertex on the 2D grid. When the weight l of the self-loop is optimally adjusted, the LQW can find the solution to the search problem in $O(\sqrt{N \log N})$ steps, which is an $O(\sqrt{\log N})$ improvement over that loopless version presented in [21].

The LQW improvement was achieved by fitting the self-loop weight to $l = 4/N$, where N is the total number of vertices. This optimal value, although, is only one instance of a general observation about the LQW searching vertex-transitive graphs with $m = 1$ solutions. For these cases, the optimal self-loop weight l equals the degree of the graph without loops (which is 4 for 2D grids) divided by N [28]. An analytical proof of this conjecture is given in [29] using the fact that the LQW can be approximated by the quantum interpolated walk.

However, that conjecture about the adjustment of l does not hold when the number of solutions m in the grid is higher than 1. Thus, another adjustment of l is required. Saha et al. [30] showed that $l = \frac{4}{N(m + \lfloor \sqrt{m}/2 \rfloor)}$ is the optimal value when m solutions are arranged as a block of $\sqrt{m} \times \sqrt{m}$ within the grid. In contrast, Nahimovs [31] demonstrated that this new adjustment

of l is not optimal for arbitrary placements of the solutions. Instead, two other adjustments were proposed, both in the form $l = \frac{4(m-O(m))}{N}$. After that, Giri and Korepin [32] showed that one of these m solutions can be obtained with sufficiently high probability in $O(\sqrt{\frac{N}{m} \log \frac{N}{m}})$ steps.

This paper is an extension of the conference paper presented in [33]. The work as a whole is an extensive experimental analysis of the LQW algorithm searching for multiple solutions on grids. By addressing several practical issues, this work contributes to the successful application of the technique. Firstly, we demonstrate that LQW simulations should stop accordingly to the stopping condition used in [26] because the stopping condition used in [31] is satisfied prematurely, i.e., when the system could evolve even further. After, we show that the final success probability is inversely proportional to the space density of solutions and directly proportional to the relative distance between solutions. However, those relations are only valid for high values of both N and m because disturbed behaviors exist in a transition between small to high values. Our results have already been corroborated and extended in the literature. Nahimovs and Santos [34] showed that the success probability is inversely proportional to the density of solutions not only on rectangular 2D grids but also on triangular and honeycomb 2D grids.

The extended material that legitimates this overall paper as a journal article is pointed out in the following. First, we generalize the LQW to search for multiple solutions on d -dimensional grids. This allows searching for solutions with an arbitrary number of dimensions. Retrieving higher than two quantities per solution is supposed to enlarge the spectrum of applications. For example, one application we glimpse is to use the LQW to search all weights and biases of artificial neural networks, inspired by the incipient work developed in [35] after consolidated in [36], which applied a lackadaisical quantum walk for complete graphs. As quantum information routing by quantum walks can benefit from high dimensional cases [13], spatial information search by quantum walks can also. For example, spatial search by quantum walks on sufficiently high dimensions can allow the full $O(\sqrt{N})$ speedup, which is unfeasible in low dimensions [8, 20]. Thus, the information that encodes the solution to the search problem may be retrieved faster.

Besides broadening the applicability of the LQW algorithm, this extended paper also addresses practical issues that appear on d -dimensional grids with multiple solutions. In this way, we propose a generalized adjustment of the self-loop weight l , which is critical to achieve success in d -dimensional grids. The other fits reported in the literature [26, 28, 31] are particular cases of our generalized value. Finally, we observe a two-to-one relation between the steps of the LQW and the steps of Grover's algorithm, which requires a modification in the stopping condition to escape numerical fluctuations in the step intermediary to the actual amplitude amplification.

This paper is organized as follows. Section 2 presents theoretical background about the task of search on 2D grids by the LQW algorithm. Here, the reader is expected to be familiar with the basics of quantum computing. If it is not the case, knowledge from the basic to the advanced levels can be obtained, for example, in [1, 37, 38, 39]. In Section 3, the different stopping conditions used in previous works are compared. After, Section 4 relates the impacts on the success probability to both the space density of solutions and the relative distance between solutions. All the findings that extend the conference version paper are presented in Section 5, which include generalizing the LQW to grids of arbitrary dimensions with multiple solutions, finding a new optimal value of l , and modifying the stopping condition to tolerate a meaningful kind of fluctuation. Finally, Section 6 presents concluding remarks.

2 Search with the Lackadaisical Quantum Walk

The classical random walk is a probabilistic movement in which a particle jumps to its adjacent positions based on the outcome of a non-biased random variable at each step [18]. Generally,

this random variable is a fair coin that has one degree of freedom for each possible direction of movement in the space at hand.

The quantum walk, in turn, is a generalized concept in comparison with the classical random walk. That high-level idea of conditioned movements remains, but quantum operations are responsible for evolving the system. In this context, quantum properties such as interference and superposition allow the quantum walk to spread quadratically faster than the classical one [18]. This advantage, therefore, can be used to search spatial regions more efficiently [40].

2.1 Spatial Search with a Quantum Walk

Ambainis et al. [21] proposed a quantum walk algorithm to search a single vertex, also called the marked vertex, in the 2-dimensional grid of $L \times L = N$ vertices. In that work, the process evolved on the Hilbert space $\mathcal{H} = \mathcal{H}_C \otimes \mathcal{H}_P$, where \mathcal{H}_C is the 4-dimensional coin space, spanned by $\{|\uparrow\rangle, |\downarrow\rangle, |\leftarrow\rangle, |\rightarrow\rangle\}$, and \mathcal{H}_P represents the N -dimensional space of positions, spanned by $\{|x, y\rangle : x, y \in [0, \dots, L-1]\}$.

Firstly, the coin toss is accomplished by the operator C presented in Equation 1, which combines the coin operators C_0 and C_1 in such a way that C_1 is applied only to the marked state $|v\rangle$, while C_0 is applied to the others. This idea of different evolution regimes for marked and unmarked vertices was introduced in [24]. Particularly, Ambainis et al. [21] defined C_0 as the Grover diffusion coin: $C_0 = 2|s\rangle\langle s| - I_4$, where $|s\rangle = \frac{1}{2}(|\uparrow\rangle + |\downarrow\rangle + |\leftarrow\rangle + |\rightarrow\rangle)$ and I_4 denotes the 4-dimensional identity operator. Finally, C_1 was defined as $-I_4$. Thus, $-I_4$ is applied to the marked state, while the Grover diffusion coin is applied to the others.

$$C = C_0 \otimes (I_4 - |v\rangle\langle v|) + C_1 \otimes |v\rangle\langle v| \quad (1)$$

Then, the flip-flop shift operator S_{ff} is applied to move the quantum particle while inverting the coin state, as presented in Equation 2. This shift works mod $\sqrt{N} = L$ because the grid has periodic boundary conditions. Finally, the quantum walk is a repeated application of the operator $U = S_{ff} \cdot C$ to the quantum system $|\psi\rangle$, which begins in the state $|\psi(0)\rangle = \frac{1}{\sqrt{N}} \sum_{x,y=0}^{\sqrt{N}-1} |s\rangle \otimes |x, y\rangle$.

$$\begin{aligned} S_{ff} |\rightarrow\rangle |x, y\rangle &= |\leftarrow\rangle |x+1, y\rangle \\ S_{ff} |\leftarrow\rangle |x, y\rangle &= |\rightarrow\rangle |x-1, y\rangle \\ S_{ff} |\uparrow\rangle |x, y\rangle &= |\downarrow\rangle |x, y+1\rangle \\ S_{ff} |\downarrow\rangle |x, y\rangle &= |\uparrow\rangle |x, y-1\rangle \end{aligned} \quad (2)$$

As a result, the marked vertex can be obtained at the measurement with a probability $O(1/\log N)$ after $T = O(\sqrt{N \log N})$ steps. To achieve a success probability near to 1, it was applied amplitude amplification [41], which implied additional $O(\sqrt{\log N})$ steps. Hence, the total running time of this quantum walk based search algorithm is $O(\sqrt{N \log N})$.

2.2 Improved Running Time by the Lackadaisical Quantum Walk

The LQW search algorithm [26] is an approach strictly based on that algorithm designed in [21] we just discussed. The main modification is to attach a self-loop of weight l at each vertex of the 2D grid, which implies other changes in the loopless technique. First, \mathcal{H}_C is spanned now by $\{|\uparrow\rangle, |\downarrow\rangle, |\leftarrow\rangle, |\rightarrow\rangle, |\odot\rangle\}$ because of the new degree of freedom. However, no changes are required for \mathcal{H}_P .

Regarding the coin operator, C_0 was defined as the Grover diffusion coin for weighted graphs [42], so $C_0 = 2|s_c\rangle\langle s_c| - I_5$, where $|s_c\rangle$ is the non-uniform distribution presented in Equation 3,

and I_5 denotes the 5-dimensional identity operator. Also, better results were found when $C_1 = -C_0$, outperforming that choice of $C_1 = -I$ used in [21]. About the shift operator S_{ff} , it works like an identity operator when applied to $|\odot\rangle|x, y\rangle$. Finally, the quantum system $|\psi\rangle$ begins in a uniform distribution between all vertices with their edges in the weighted superposition $|s_c\rangle$ instead of the uniform $|s\rangle$.

$$|s_c\rangle = \frac{1}{\sqrt{4+l}}(|\uparrow\rangle + |\downarrow\rangle + |\leftarrow\rangle + |\rightarrow\rangle + \sqrt{l}|\odot\rangle) \quad (3)$$

As a result, the LQW with $l = 4/N$ finds the marked vertex with a success probability close to 1 after $T = O(\sqrt{N \log N})$ steps. This is an $O(\sqrt{\log N})$ improvement over the loopless algorithm. More sophisticated approaches have also achieved this improvement in running time [43, 44, 45], but the LQW is a significantly simpler and equally capable technique. Moreover, the success probability converges closer and closer to 1 if the number of vertices N increases when using that optimal l .

Those numerical results reported in [26] were found by simulations that stopped when the first peak in the success probability occurred. For that, the stopping condition monitored the success probability at each step. When the current value was smaller than the immediately previous one for the first time, the simulation stopped, and this immediately previous result was reported as the maximum found.

2.3 Lackadaisical Quantum Walk with Multiple Solutions

If there are multiple marked vertices, i.e., multiple solutions in the search space, the LQW results for the case with only one solution do not hold. Significant research efforts have focused on adjusting the weight l optimally for such cases with multiple solutions. For instance, Saha et al. [30] addressed m marked vertices arranged as a block of $\sqrt{m} \times \sqrt{m}$ within a $\sqrt{N} \times \sqrt{N}$ grid, as already studied for the loopless version in [46]. In this scenario of block arrangements, the LQW can produce success probabilities that exceed 0.95 for large values of N with the optimal weight value of $l = \frac{4}{N(m + \lfloor \sqrt{m}/2 \rfloor)}$ [30]. However, these results do not hold if the solutions are randomly sampled, as Nahimovs [31] demonstrated. A new choice of l is required.

Thereby, Nahimovs [31] searched for new optimal values in the form $l = \frac{4}{N} \cdot a$. Thus, l was adjusted as a factor of the optimal value for $m = 1$ reported in [26], which was $l = 4/N$. As a result, two adjustments were proposed: $l = \frac{4m}{N}$, for small values of m , and $l = \frac{4(m - \sqrt{m})}{N}$, for large values of m . To find these optimal values of l , the m solutions were arranged following the M_m set presented in Equation 4. However, random placements of solutions yielded similar results.

$$M_m = \{(0, 10i) \mid i \in [0, m - 1]\} \quad (4)$$

Regarding the simulations performed in [31], a different stopping condition was used rather than monitoring the success probability at each step. Alternatively, the inner product $|\langle \psi(t) | \psi(0) \rangle|$ was monitored until its minimum is achieved, so the simulation stopped when this inner product became close to 0 in absolute value for the first time since the process is periodic.

3 Comparison between Different Stopping Conditions

It is possible to find two stopping conditions in the literature regarding the LQW simulations. One of them is to monitor the success probability until its maximum is achieved [26], where success probability refers to the probability of measure a marked vertex (a solution to the search

Table 1: Convergence step T and final success probability Pr , as the number of solutions m increases, for the different stopping conditions used in previous works.

m	Stopping Conditions			
	Marked Vertices		$ \langle\psi(t) \psi(0)\rangle $	
	T	Pr	T	Pr
1	399	0.140828	420	0.138489
5	409	0.878178	288	0.593276
10	297	0.867440	249	0.704010
15	290	0.835395	254	0.747045
20	288	0.818635	268	0.778724

problem). Here, we name this stopping condition as ‘‘Marked Vertices’’. The other stopping condition is to monitor the inner product $|\langle\psi(t)|\psi(0)\rangle|$ until its minimum is achieved [31]. However, as the convergence of those stopping conditions have not been compared yet, their interchangeability became an open question. Therefore, before conducting further experimental analysis of the LQW search algorithm, we verified here whether or not those conditions converge to the same points from equal initial settings.

We made experiments using a setup equal to the one used in [31], i.e., a grid of 200 x 200 vertices with the m solutions following the M_m set. Constrained by this M_m scheme, up to 20 solutions can be placed in that space, since $M_{20} = \{(0, 0), (0, 10), \dots, (0, 180), (0, 190)\}$. Placing more than 20 solutions in the 200 x 200 grid would require a organization other than the M_m set to not extrapolate the grid limits. However, as we used the M_m scheme, we made experiments with 1, 5, 10, 15 and 20 solutions in the grid.

As a result, the stopping conditions converged to the same points for $l = \frac{4m}{N}$. However, it is not the case for $l = \frac{4(m-\sqrt{m})}{N}$, as presented in Table 1, which contrasts the results obtained monitoring the marked vertices against the ones obtained monitoring the inner product $|\langle\psi(t)|\psi(0)\rangle|$. As can be seen, the results tend to converge to the same points as m increases. Nevertheless, the conditions were not equivalent because each one was satisfied at a different step T , which implied different final success probabilities Pr as well. Also, monitoring the inner product $|\langle\psi(t)|\psi(0)\rangle|$ generated inferior success probabilities in all cases.

To investigate the divergence carefully, the system evolution step by step was stored. Figure 1 shows the evolution of the $m = 5$ case, which has the most significant discrepancy in Table 1. The black solid line represents the condition that monitors the marked vertices, while the blue dashed line represents the one that monitors the inner product $|\langle\psi(t)|\psi(0)\rangle|$.

As reported in Table 1, the condition that monitors the inner product in absolute value is satisfied prematurely at the step $T = 288$. It is said premature because the success probability continues increasing afterward, until $T = 409$. After the step $T = 288$, though, the curves have a similar growth damping, which raised a question about monitoring the real value of the inner product rather than its absolute value.

Figure 2 shows the system evolution during 1000 steps. As before, the monitoring of the marked vertices is represented by the black solid line. At this time, the inner product is monitored without calculating its absolute value, which is represented by the green dashed line. Note that the both curves have the same behavior. Therefore, it is possible to conclude that the stopping conditions used in previous works are equivalent if, and only if, the inner product is considered without calculating its absolute value. Otherwise, only the condition that monitors the marked vertices leads to the real amplitude amplification achieved by the LQW search algorithm.

In this manner, all results that will be discussed in this work from now on were found using

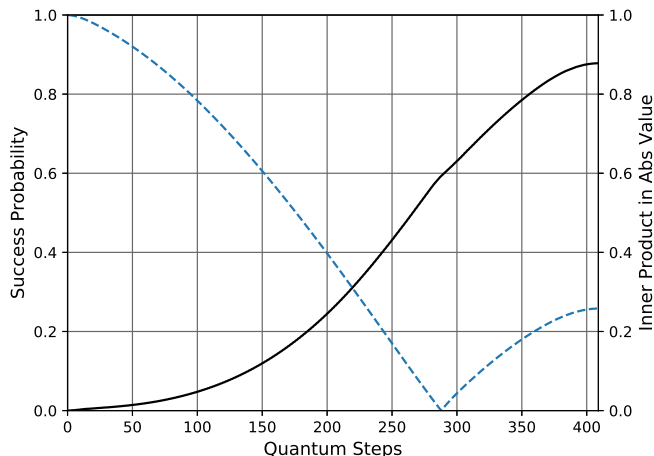


Figure 1: System evolution step by step until the condition that monitors the marked vertices is satisfied. The black solid line represents the monitoring of that condition, while the blue dashed line represents the monitoring of the inner product in absolute value.

the stopping condition that monitors the marked vertices. Since the objective is to measure the quantum system when the maximum amplification in the success probability occurs, monitoring the marked vertices is the most natural choice to define the moment when the simulation should stop.

4 Solution Setups Affecting the Success Probability

In Section 3, we analyzed the evolution of the LQW in order to verify whether the different stopping conditions would be interchangeable or not. After choosing the stopping condition properly, we now move forward to addressing factors that affect the final success probability achieved by the technique. Previous works have already demonstrated the considerable dependence of the LQW algorithm on the self-loop weight l [26, 30, 31]. Expanding those analysis, we address here the density of solutions and the relative distance between solutions.

4.1 Previous Evaluations about Space Densities of Solutions and a Complementary Experiment

The experiments performed by Wong [26] and Nahimovs [31] can reveal some dependence between the success probability and the space density of solutions ρ , where $\rho = \frac{m}{N}$. However, such works did not make links between the density of solutions and the success probability achieved at the end of the simulation. Here, we discuss these previous experiments briefly but aiming to identify the impacts of ρ . Finally, a complementary experiment was made.

Firstly, Wong [26] investigated the impacts of adding more unmarked vertices in a grid with only one solution. Actually, that experiment evaluated how decreases in density of solutions could affect the final success probability. As a result, the success probability tends to improve, even though some disturbed behavior for the first values of N exists.

After that, Nahimovs [31] inserted more and more solutions in the 200 x 200 grid when adjusting the value of l for multiple marked vertices. Since the grid size was fixed, that experiment

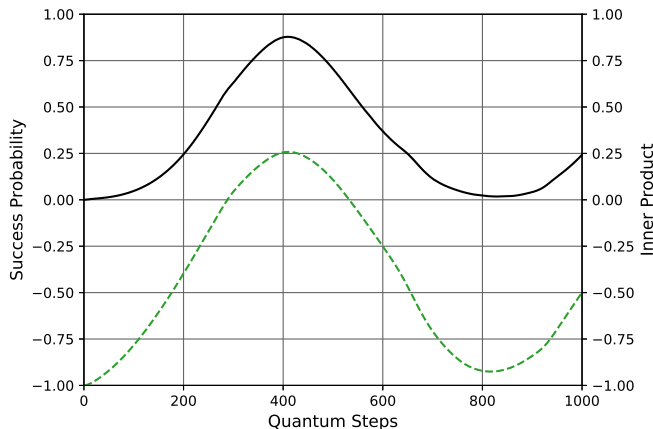


Figure 2: System evolution step by step during 1000 steps. The black solid line represents the monitoring of the marked vertices, while the green dashed line represents the monitoring of the inner product without calculating its absolute value.

increased the density of solutions with each new vertex being marked. However, the probability of measure a marked vertex was smaller when m increased. It would be a counter-intuitive idea in a classical world.

It is possible to comprehend the dependence between the total number of vertices N , the number of solutions m , and the final success probability observing the Grover algorithm [18]. Consider $|\omega\rangle$ as the state where the total energy of the quantum system is equally distributed only between the marked states, so the success probability is 1. The goal of Grover's algorithm is to rotate the state of the system $|\psi\rangle$ to get as close to $|\omega\rangle$ as possible. However, this is an iterative process in which $|\psi\rangle$ rotates at each step by an angle θ . As θ is inversely proportional to N , increasing N implies more steps T , but these fine rotations turn $|\psi\rangle$ closer to $|\omega\rangle$ as N increases, explaining the results of Wong [26]. As θ is proportional to m , increasing m implies fewer steps T if $N \gg m$, although $|\psi\rangle$ gets less close to $|\omega\rangle$ at the end, explaining the smaller success probabilities in the experiments of Nahimovs [31] while m increased.

Thus, these previous experiments suggest the success probability is inversely proportional to the density of solutions within the grid. That is in accordance with having a more refined or less refined angle θ in Grover's rotations, as explained. In this work, a complementary experiment was made to fill the gap not addressed by those previous works: how decreases in density of solutions, like in [26], can affect the LQW algorithm with multiple marked vertices, like in [31]. While we conducted that experiment, we also searched for the optimal value of l in the form $l = \frac{4}{N}a$, like in [31] again.

Figure 3 shows the peaks in the success probability, represented by the black solid line, and the optimal a values that generated these peaks, represented by the brown dashed line, both as functions of N . The density of solutions decreased in this case because m was always equal to 10, while N increased by the addition of unmarked vertices. Moreover, the optimal a values were searched with steps size of 0.5 and N varied from 10^4 to 10^6 with the $m = 10$ solutions following the M_{10} set.

Again, there is a disturbed behavior for the first N values, like in [26]. Afterward, the success probability tends to 1 as well as the optimal a value tends to the number of solutions $m = 10$. This experimental result suggest the construction $l = \frac{4(m-O(m))}{N}$ proposed in [31] is a way of adjusting for the cases where density of solutions is not small enough, because a equals m in the

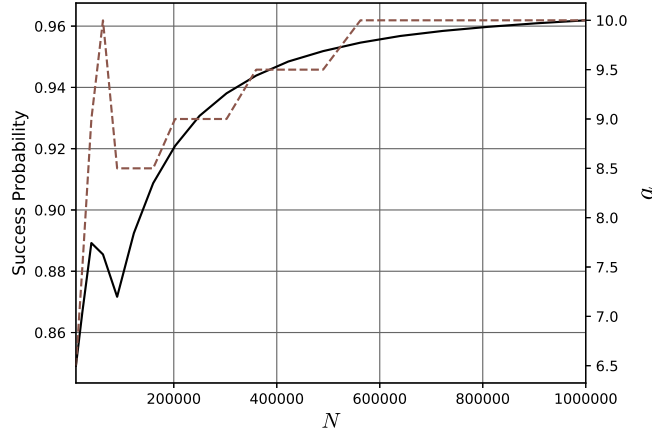


Figure 3: Peaks in the success probability (black solid line) and respective optimal a values (brown dashed line), both as functions of N , with the $m = 10$ solutions located in the 2D grid according to the M_{10} set.

best cases of solutions density and, consequently, $l = \frac{4m}{N}$.

4.2 A New Set of Solutions Increasing Relative Distances

In the last experiment, the $m = 10$ solutions were located always at the points $\{(0, 0), (0, 10), \dots, (0, 90)\}$, following the M_{10} set. That distribution of solutions did not take advantage of the gradual increment on the total number of vertices N . If the solutions were located farther away from each other, it would be possible to continue evaluating how the success probability depends on the density of solutions but also on the relative distance between solutions.

Thus, we propose an alternative to the M_m set that is the $P_{L,m}$ set presented in Equation 5. Following this new set, the m solutions are located depending on the number of vertices in each dimension L so that the grid size is better used. For example, $m = 10$ solutions on the 200×200 grid would be located at the points $\{(0, 0), (20, 20), \dots, (180, 180)\}$, following the $P_{200,10}$ set. As a consequence, the solutions are farther apart using the $P_{L,m}$ set than using the M_m set.

$$P_{L,m} = \left\{ \left(\left\lfloor \frac{L}{m} \right\rfloor i, \left\lfloor \frac{L}{m} \right\rfloor i \right) \mid i \in [0, m - 1] \right\} \quad (5)$$

Then, our complementary experiment that evaluated decreases in density of solutions with $m = 10$ solutions was redone, but using the $P_{L,m}$ set this time for localizing the solutions farther from each other. The results obtained with this new set of solutions are contrasted in Table 2 with the ones obtained previously, which used the M_m set. The success probabilities in Table 2 for the M_m set are exactly the ones already presented in Figure 3 but in terms of L now because L is the variable used to define the $P_{L,m}$ set. It is worth reminding that $L^2 = N$.

For all values of L , the set of solutions $P_{L,m}$ generated better results because the success probability was higher and with a smaller number of steps. Besides this, the disturbed behavior for the first values of L did not appear in the results with the new set of solutions. Finally, it is possible to conclude from these numerical results that the success probability is directly proportional to the relative distance between solutions.

Table 2: Number of steps and final success probabilities as L increases for different sets of $m = 10$ solutions.

L	$M_{m=10}$		$P_{L,m=10}$	
	T	Pr	T	Pr
100	147	0.849178	109	0.902339
200	293	0.889219	223	0.927680
300	511	0.871665	342	0.940301
400	747	0.908749	460	0.948348
500	965	0.930714	581	0.953927
600	1181	0.943863	700	0.958288
700	1407	0.951843	822	0.961646
800	1623	0.956787	941	0.964317
900	1857	0.959761	1063	0.966613
1000	2097	0.961896	1187	0.968522

Table 3: Values of m that do not have asymptotic and growing behaviors for the success probability as the density of solutions decreases.

L	Pr		
	$m = 3$	$m = 4$	$m = 5$
100	0.991433	0.986119	0.981772
200	0.988165	0.992391	0.990397
300	0.985744	0.993451	0.992697
400	0.984221	0.993206	0.993754
500	0.983418	0.992604	0.994283
600	0.983100	0.991933	0.994585
700	0.983081	0.991282	0.994717
800	0.983252	0.990683	0.994677
900	0.983548	0.990138	0.994557
1000	0.983927	0.989644	0.994392

Regardless of whether or not a disturbed behavior exists for the first L values, the success probability had an asymptotic and growing behavior for higher values of L in all previous cases discussed here. However, that is not true for all values of m . Table 3 shows the same investigation of decreases in density of solutions with the $P_{L,m}$ set again, but for $m = \{3, 4, 5\}$, and not for $m = 10$ as before.

The qualitative behaviors found for these m values are not equal to the behaviors for both $m = 1$, as reported in [26], and $m = 10$, as shown in Figure 3 and Table 2. In those $m = 1$ and $m = 10$ cases, a disturbed behavior existed during a transition from small to high values of L and, then, the success probability improved continuously. However, $m = \{3, 4, 5\}$ can be seen as a kind of transition from small to high values as well but from the perspective of the number of solutions m . It suggests that the asymptotic and growing behavior for the success probability as density of solutions decreases is only guaranteed for values high enough of both $L = \sqrt{N}$ and m .

4.3 Evaluation of Density Increasing with the New Set of Solutions

In fact, the density of solutions within the grid affects the final success probability achieved by the LQW algorithm. We already analyzed decreases in density of solutions by the addition of

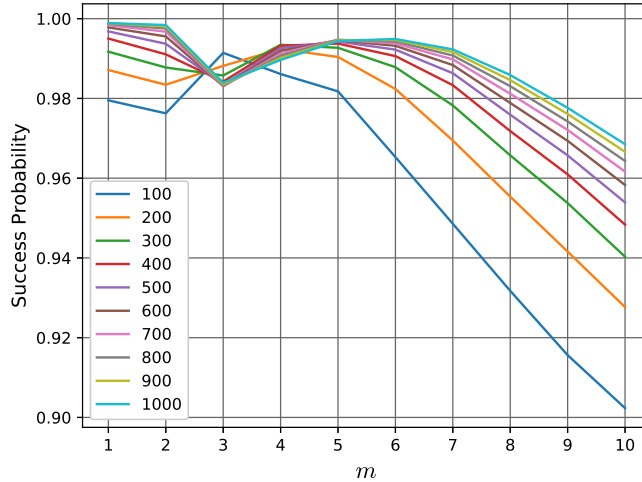


Figure 4: Final success probability as density of solutions increases with the solutions following the $P_{L,m}$ set. The colored lines represent grids with different numbers L of vertices per dimension.

unmarked vertices using both the M_m and $P_{L,m}$ sets. Regarding increases in density of solutions, we complement this analysis here using the $P_{L,m}$ set since results using the M_m set are found in [31]. Increases in density of solutions occur by having more marked vertices in a grid of fixed size $L \times L$.

Figure 4 shows the final success probability as a function of the number of solutions m for grids with different numbers L of vertices per dimension. The colored lines represent the results for grids with L varying from 100 to 1000 and with the number of solutions $m = \{1, 2, \dots, 10\}$ following the $P_{L,m}$ set.

As expected, because of the inversely proportional relation, the success probability decreases as the density of solutions increases by having more solutions in the grid. However, these results with the $P_{L,m}$ set also had that transitory phenomenon. For all cases, there are intervals where a disturbed behavior exists and, then, the success probability tends to decrease continuously.

This was one more perspective showing some uncertainty about the behavior of the LQW algorithm with small values of some input parameter. Thus, it is more confident to apply the LQW search algorithm in real scenarios where the input parameters are higher to avoid those disturbed behaviors presented in this work.

5 Lackadaisical Quantum Walk on d-dimensional Grids

In this section, we present the extension of the work developed in [33]. The novelties deal with the application of the LQW algorithm on grids of arbitrary dimensions with multiple solutions. Also, we address issues regarding the successful application of the technique in such new scenarios.

When a vertex is marked as a solution in the two-dimensional case, it means that the vertex's coordinates x and y , combined, satisfy the search problem, whatever the search problem is. Searching and retrieving only two values can be seen as a limitation because more than two quantities may be required to solve some applications. The idea here is to expand the technique to search for solutions with an arbitrary number of dimensions, which implies walking through grids with higher than two dimensions. The new capacity is supposed to expand the spectrum

of applications of the LQW search algorithm.

In the following, the mathematical formalism is redefined, new implications regarding classical simulations are discussed, the self-loop weight l is adjusted, and the stopping condition is revisited, all of this considering issues that arise in scenarios with arbitrary dimensions.

5.1 Generalization to d-dimensional Grids

Here, the mathematical formalism is rewritten to the search with the LQW algorithm on grids of higher dimensions. Fortunately, the generalization is straightforward from the two-dimensional formulation, which is demonstrated in the following algebra. Besides that, we discuss some aspects involving classical simulations of the technique generalized to grids of arbitrary dimensions.

Considering a grid with d dimensions, each vertex has $2*d+1$ possible directions of movement because each dimension has a positive and a negative direction, and there is a self-loop attached to the vertex. In a generalized way, the coin space \mathcal{H}_C is spanned by $\{|\uparrow_1\rangle, |\downarrow_1\rangle, \dots, |\uparrow_d\rangle, |\downarrow_d\rangle, |\odot\rangle\}$, where \uparrow_i and \downarrow_i represent the movements on the i -th dimension. The computational basis for the space of positions \mathcal{H}_P is $\{|x_1, \dots, x_d\rangle : x_i \in [0, \dots, \sqrt[d]{N} - 1]\}$. Thus, the quantum walk evolve on the space $\mathcal{H} = \mathcal{H}_C \otimes \mathcal{H}_P$ with these generalized reformulations.

Marking a vertex by applying $C_1 = -C_0$, while only C_0 is applied to non-solution vertices, can be replaced by an oracle that is applied first and then C_0 acts over all states. Since the oracle flips the sign of all m marked vertices, the overall effect is the application of $-C_0$ to the marked vertices and C_0 itself to the others. Using an oracle, C does not need to be broken down into two different coin operators, so $C = C_0$. In a generalized form, the coin operator C is now defined as presented in Equation 6, which uses the generalized distribution $|s_c\rangle$ presented in Equation 7.

$$C = 2|s_c\rangle\langle s_c| - I_{2d+1} \quad (6)$$

$$|s_c\rangle = \frac{1}{\sqrt{2*d+l}}(|\uparrow_1\rangle + |\downarrow_1\rangle + \dots + |\uparrow_d\rangle + |\downarrow_d\rangle + \sqrt{l}|\odot\rangle) \quad (7)$$

Consider this coin operator C applied in such generic superposition $|\phi\rangle = (\alpha_1, \alpha_2, \dots, \alpha_{2d-1}, \alpha_{2d}, \alpha_{2d+1})^T$, representing any state of the generalized coin space \mathcal{H}_C . For this purpose, the outer product $|s_c\rangle\langle s_c|$ can be more detailed as follows:

$$\begin{aligned} |s_c\rangle\langle s_c| &= \frac{1}{\sqrt{2*d+l}} \begin{pmatrix} 1 \\ 1 \\ \vdots \\ 1 \\ 1 \\ \sqrt{l} \end{pmatrix} * \frac{1}{\sqrt{2*d+l}} (1 \quad 1 \quad \dots \quad 1 \quad 1 \quad \sqrt{l}) \\ &= \frac{1}{2*d+l} \begin{pmatrix} 1 & 1 & \dots & 1 & 1 & \sqrt{l} \\ 1 & 1 & \dots & 1 & 1 & \sqrt{l} \\ \vdots & \vdots & \vdots & \vdots & \vdots & \vdots \\ 1 & 1 & \dots & 1 & 1 & \sqrt{l} \\ 1 & 1 & \dots & 1 & 1 & \sqrt{l} \\ \sqrt{l} & \sqrt{l} & \dots & \sqrt{l} & \sqrt{l} & l \end{pmatrix}. \end{aligned}$$

Thus, the application of the coin operator C in that generic state is as follows:

$$\begin{aligned}
& (2|s_c\rangle\langle s_c| - I_{2d+1})|\phi\rangle = 2|s_c\rangle\langle s_c|\phi\rangle - I_{2d+1}|\phi\rangle \\
& = 2 * \frac{1}{2 * d + l} \begin{pmatrix} 1 & 1 & \dots & 1 & 1 & \sqrt{l} \\ 1 & 1 & \dots & 1 & 1 & \sqrt{l} \\ \vdots & \vdots & \vdots & \vdots & \vdots & \vdots \\ 1 & 1 & \dots & 1 & 1 & \sqrt{l} \\ 1 & 1 & \dots & 1 & 1 & \sqrt{l} \\ \sqrt{l} & \sqrt{l} & \dots & \sqrt{l} & \sqrt{l} & l \end{pmatrix} \begin{pmatrix} \alpha_1 \\ \alpha_2 \\ \vdots \\ \alpha_{2d-1} \\ \alpha_{2d} \\ \alpha_{2d+1} \end{pmatrix} - \begin{pmatrix} 1 & 0 & \dots & 0 & 0 & 0 \\ 0 & 1 & \dots & 0 & 0 & 0 \\ \vdots & \vdots & \vdots & \vdots & \vdots & \vdots \\ 0 & 0 & \dots & 1 & 0 & 0 \\ 0 & 0 & \dots & 0 & 1 & 0 \\ 0 & 0 & \dots & 0 & 0 & 1 \end{pmatrix} \begin{pmatrix} \alpha_1 \\ \alpha_2 \\ \vdots \\ \alpha_{2d-1} \\ \alpha_{2d} \\ \alpha_{2d+1} \end{pmatrix} \\
& = 2 * \frac{1}{2 * d + l} \begin{pmatrix} \alpha_1 + \alpha_2 + \dots + \alpha_{2d-1} + \alpha_{2d} + \sqrt{l} * \alpha_{2d+1} \\ \alpha_1 + \alpha_2 + \dots + \alpha_{2d-1} + \alpha_{2d} + \sqrt{l} * \alpha_{2d+1} \\ \vdots \\ \alpha_1 + \alpha_2 + \dots + \alpha_{2d-1} + \alpha_{2d} + \sqrt{l} * \alpha_{2d+1} \\ \alpha_1 + \alpha_2 + \dots + \alpha_{2d-1} + \alpha_{2d} + \sqrt{l} * \alpha_{2d+1} \\ \sqrt{l} * (\alpha_1 + \alpha_2 + \dots + \alpha_{2d-1} + \alpha_{2d} + \sqrt{l} * \alpha_{2d+1}) \end{pmatrix} - \begin{pmatrix} \alpha_1 \\ \alpha_2 \\ \vdots \\ \alpha_{2d-1} \\ \alpha_{2d} \\ \alpha_{2d+1} \end{pmatrix}.
\end{aligned}$$

Defining λ as:

$$\lambda = \frac{1}{2 * d + l} (\alpha_1 + \alpha_2 + \dots + \alpha_{2d-1} + \alpha_{2d} + \sqrt{l} * \alpha_{2d+1}),$$

the application of the coin operator C comes down to:

$$(2|s_c\rangle\langle s_c| - I_{2d+1})|\phi\rangle = \begin{pmatrix} 2 * \lambda - \alpha_1 \\ 2 * \lambda - \alpha_2 \\ \vdots \\ 2 * \lambda - \alpha_{2d-1} \\ 2 * \lambda - \alpha_{2d} \\ 2 * \lambda * \sqrt{l} - \alpha_{2d+1} \end{pmatrix}.$$

This is exactly the result expected when the weighted Grover diffusion coin is applied. Since λ is not the mean of the coin amplitudes, the inversion is about a mean that takes into account the weight of the graph edges rather than the simple arithmetic mean [42]. And all this worked out in the generalized form.

Regarding classical simulations, the coefficients $\alpha_1, \dots, \alpha_{2d}$ must be handled in a flexible and generalized way according to the total number of dimensions, besides considering the loop's weight appropriately to normalize the quantum state. It turns out that the simulation is similar to the one developed by Wong [26], but considering the generalized relations stated here when it comes to the coin operator.

About the flip-flop shift operator S_{ff} , there is also no restriction to generalize it. The intuition behind this operator is to transfer energy between vertices in a dimension-per-dimension way. At a step, what is happening in one dimension for a vertex does not affect what is happening in

Table 4: Number of steps and final success probability for some cases in grids with higher than two dimensions using $l = \frac{4m}{N}$ and the $P_{d,L,m}$ set.

d	L	m	T	Pr
3	32	8	134	0.958805
4	16	4	257	0.888795
5	10	5	285	0.816259
6	8	4	441	0.739591

another dimension for the same vertex. For example, in each step, a vertex $|v\rangle$ stores on its state $|\uparrow_i\rangle$ the energy coming from the state $|\downarrow_i\rangle$ of the vertex immediately following on the direction \uparrow_i , and vice versa. Note that, for that dimension, the others do not cause interference.

Therefore, all that is required for generalizing is to operate, dimension by dimension, as presented in Equation 8. That pattern of dimension-wise energy transfer simplifies an abstraction for a classical simulation. In each step, through a double for-loop, the implementation can replicate the operation in each dimension one-by-one for each vertex.

$$\begin{aligned} S_{ff} |\uparrow_i\rangle |x_1, \dots, x_i, \dots, x_d\rangle &= |\downarrow_i\rangle |x_1, \dots, x_i + 1, \dots, x_d\rangle \\ S_{ff} |\downarrow_i\rangle |x_1, \dots, x_i, \dots, x_d\rangle &= |\uparrow_i\rangle |x_1, \dots, x_i - 1, \dots, x_d\rangle \end{aligned} \quad (8)$$

As before, the energy stored in the self-loop remains unchanged after an application of the flip-flop shift operator, i.e., $S_{ff} |\odot\rangle |x_1, \dots, x_i, \dots, x_d\rangle = |\odot\rangle |x_1, \dots, x_i, \dots, x_d\rangle$. Thus, no considerations are needed for generalization. As the space topology is torus-like because of the periodic boundary conditions, the shift operates mod $\sqrt[d]{N}$.

Finally, the system begins in the uniform distribution between each of the N vertices of the d -dimensional grid with the weighted superposition of coin states generalized in Equation 7. The step where the simulation stops depends on a stopping condition, but the more appropriate one is to monitor the probability's evolution about the m marked vertices until achieving its maximum [33]. Now, the LQW algorithm can be simulated on higher-than-two-dimensional grids with multiple solutions.

5.2 Application on d-dimensional Grids

In real applications, the solutions could be at any grid point. However, for methodological reasons, the experiment setup is controlled in terms of solutions' positions [26, 31, 33]. It is not different here. To conduct our experiments, we locate the m solutions according the $P_{d,L,m}$ set presented in Equation 9, which is a straightforward generalization of the $P_{L,m}$ set already introduced in Equation 5. Therefore, each solution is a d -tuple, and the solutions are located equidistantly on the grid's main diagonal.

$$P_{d,L,m} = \left\{ \left(\left\lfloor \frac{L}{m} \right\rfloor i, \dots, \left\lfloor \frac{L}{m} \right\rfloor i \right)_d \mid i \in [0, m-1] \right\} \quad (9)$$

Since the technique, the stopping condition, and the solution setup are described, experiments can be performed on grids of higher dimensions. The number of steps T and the final success probability Pr for the investigated d -dimensional cases are presented in Table 4. Note that the success probability decreases as the number of dimensions increases, suggesting the LQW algorithm tends to be ineffective in higher-than-two-dimensional scenarios.

Although L and m varied in the cases presented in Table 4, the density of solutions was small enough and the relative distance between solutions was high enough to not affect substantially

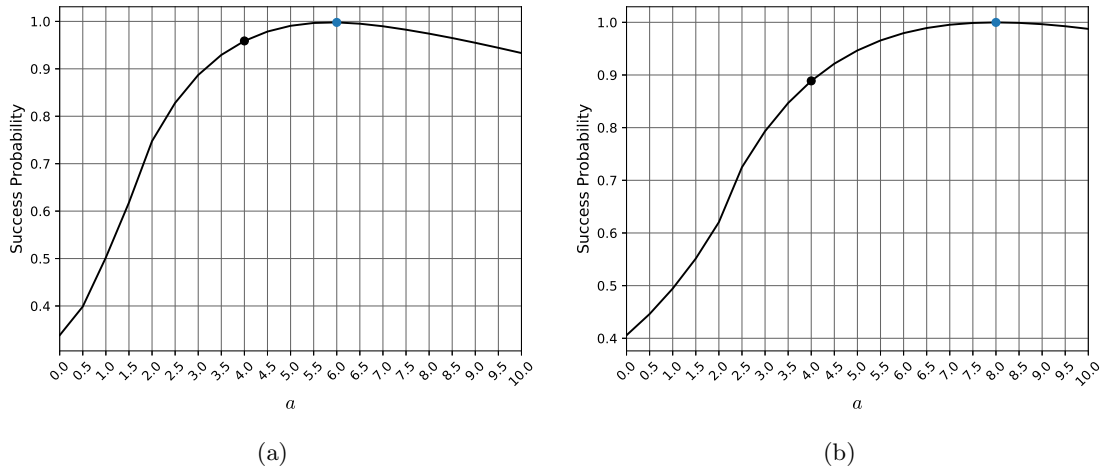


Figure 5: Final success probability as a function of a for the self-loop weight in the form $l = \rho * a$. To the left, results for the 3D case with $L = 32$ and $m = 8$. To the right, results for the 4D case with $L = 16$ and $m = 4$. The black dot marks the results for a equal to 4, while the blue dot marks the best overall result found.

at all. Thus, the final success probability deteriorated strictly due to increases in the number of dimensions d . Those results were found setting $l = \frac{4m}{N}$ for being the optimal l on 2D grids, at least for the best cases of solution densities. However, it makes room to search for even better adjustments of the self-loop weight l as research efforts already demonstrated how critical to adjust it is [26, 30, 31]. The objective of the following experiment is to verify whether another optimal value of l for d higher than two exists or not.

As demonstrated in [26], l is inversely proportional to the number of vertices N . At the same time, l is directly proportional to the number of solutions m [31]. Thus, the value of l depends on the density of solutions ρ , where $\rho = \frac{m}{N}$. Preserving the relations found by those works, we search for new fits of l in the form $l = \rho * a$, where a is a multiplicative factor. From those previous works, the value of a would be 4, which deteriorated performance when d increased in Table 4.

Figure 5a and Figure 5b show the final success probability as a function of that multiplicative factor a for the 3D and 4D cases presented in Table 4, respectively. The result for $a = 4$ is marked by the black dot, while the best overall result found in the search is marked by the blue dot. In both cases, $a = 4$ is not the optimal value because other values generated better success probabilities. The best result found in the search could generate success probabilities near to 1, while its distance to the $a = 4$ gets larger when d increases.

Regarding the other cases presented in Table 4, the best overall results found in the search generated success probabilities of 0.999933 for the 5D case and 0.999986 for the 6D case. In this way, it is possible to conclude that the LQW algorithm can generate satisfactory results when applied in grids with higher than two dimensions with multiple solutions. The results reported in Table 4 deteriorated because a equal to 4, which was proposed by previous works, is optimal only in the restricted 2D case.

Moreover, our results revealed a pattern. The best values of a found in the search were 6 for the 3D case, 8 for the 4D case, 10 for the 5D case, and 12 for the 6D case. Thus, the experimental results suggest that the optimal value of a is $2 * d$, so the optimal value of l for d -dimensional grids is $l = \rho * 2d = \frac{2dm}{N}$. In the 2D case, $l = \rho * 2 * 2 = \frac{4m}{N}$, as proposed in previous works.

Table 5: Number of steps and final success probability for some d -dimensional grids using the value of l proposed in previous works, $l = \frac{4m}{N}$, and the value proposed in this work, $l = \frac{2dm}{N}$.

d	L	m	$l = \frac{4m}{N}$		$l = \frac{2dm}{N}$	
			T	Pr	T	Pr
3	32	4	187	0.959003	171	0.999531
3	64	8	381	0.959096	348	0.999736
4	16	2	364	0.888818	315	0.999912
4	30	3	1048	0.88888	907	0.99999
5	10	2	453	0.816318	377	0.999982
5	15	5	784	0.816322	658	0.999991
6	8	2	593	0.731387	600	0.999994
6	10	10	541	0.73811	525	0.999986
7	6	6	388	0.692785	354	0.99999
8	4	2	247	0.637346	295	0.999979

Table 6: Number of steps and final success probability for d -dimensional cases that prematurely stopped using both the value of l proposed in previous works, $l = \frac{4m}{N}$, and the value proposed in this work, $l = \frac{2dm}{N}$.

d	L	m	$l = \frac{4m}{N}$		$l = \frac{2dm}{N}$	
			T	Pr	T	Pr
5	10	2	24	0.009348	24	0.009374
5	15	3	24	0.001847	24	0.001848
5	15	5	14	0.001108	14	0.001108
7	6	6	6	0.000878	6	0.000878

More experimental evidence is presented in Table 5, which compares results obtained using the l proposed in previous works ($l = \frac{4m}{N}$) with the ones obtained using the l proposed in this work ($l = \frac{2dm}{N}$), for a variety of cases in higher than two dimensions.

For all cases, $l = \frac{2dm}{N}$ generated success probabilities near to 1, while $l = \frac{4m}{N}$ generated inferior results that deteriorated further as d increased. For the cases presented in Table 5, not only experiments with those two fits of l were made, but no other adjustment surpassed the result of using $l = \frac{2dm}{N}$, indicating that it is the optimal value for d -dimensional grids with multiple solutions, in fact.

5.3 Stopping Condition Revisited

As demonstrated in [33], the more appropriate and natural choice of stopping condition is to monitor the probability evolution about the m marked vertices until this quantity achieves its maximum. The maximum is determined by finding a step whose success probability is smaller than the immediately previous one. That approach assumes a function that increases monotonically, achieves its maximum, and decreases monotonically after that maximum. However, it is not the case in some examples on grids with higher than two dimensions.

Table 6 shows four special cases that stopped at a considerably premature step by using as criterion finding a step whose success probability is smaller than the immediately previous one. Regardless of the value of l , each case stopped at the same premature step and, consequently, with an extremely unsatisfactory success probability.

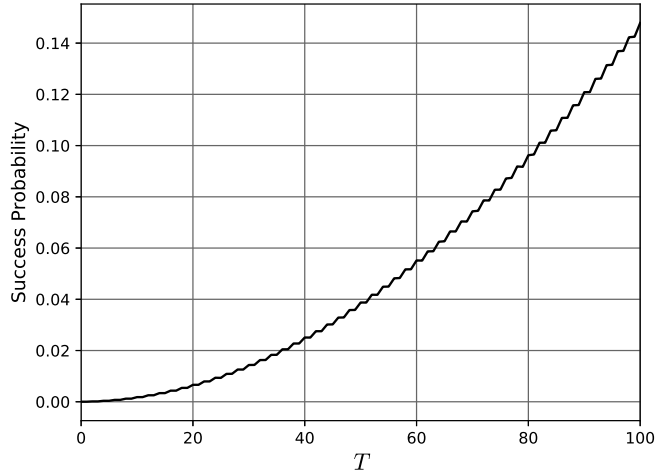


Figure 6: Success probability during the first 100 steps on the 5D grid with $L = 10$, $m = 2$ and the value of l proposed in this work, which is $l = \frac{2dm}{N}$.

Figure 6 shows the system’s evolution during 100 steps for the first case presented in Table 6, which is the 5D grid with $L = 10$ and $m = 2$. This experiment intended to evaluate whether or not the system can evolve further, even though the stopping condition is satisfied too early. Qualitatively, as can be seen, the success probability improves continuously as more steps are performed, but there is a kind of fluctuation in the process. However, this fluctuation has a meaning.

Ambainis et al. [21] mathematically proved that two steps of a particular quantum walk search algorithm give exactly one step of Grover’s algorithm. It turns out, in every two steps, the first is an intermediary step to the actual amplitude amplification generated by the second step of the quantum walk. That quantum walk occurred on a complete graph with a non-weighted self-loop for each vertex.

The result we showed in Figure 6 is supposed to be an experimental demonstration of that two-to-one relation between quantum walks and Grover’s algorithm steps. The interesting here is that we used a quantum walk with weighted self-loops on grids with higher than two dimensions, and not a quantum walk with non-weighted self-loops on a complete graph as used in [21]. Nevertheless, there are similarities, because both quantum walk approaches apply a Grover diffusion coin and the flip-flop shift operator S_{ff} , subsequently.

The practical implication in terms of stopping condition is simply not to compare success probabilities between adjacent steps, because one of them is an intermediary step subject to fluctuations, as shown explicitly in Figure 6. Instead of comparing with the immediately previous step, the solution is to compare with the penultimate step.

In this way, the simulation stops in the step whose success probability is smaller than the one of the penultimate step, and the success probability of that penultimate step is reported as the maximum found. This is enough to conceive a more robust stopping condition capable of escaping the premature stops reported in Table 6. To obtain those results reported in Table 5, especially for these special cases, the stopping condition needs this slight modification.

6 Final Remarks

This paper is an extended version of a conference paper. The overall research addressed the LQW search algorithm and its capabilities from an experimental point of view. We aimed to understand more clearly properties and existing limitations, in addition to giving contributions to conceive a better quantum-walk-based solver of search problems.

In this way, first, we demonstrated that different stopping conditions used in previous works are not interchangeable. Calculating the absolute value of the inner product $\langle\psi(t)|\psi(0)\rangle$ implies prematurely stops. Rather, the real value must be used. After choosing the stopping condition properly, we demonstrated that the final success probability is inversely proportional to the density of solutions and directly proportional to the relative distance between solutions. However, those relations are guaranteed only for high values of the input parameters. From different perspectives, we showed a disturbed behavior in a transition between small to high values of the input parameters.

Regarding the findings that extend the work, we generalized the LQW algorithm to search for multiple solutions on grids of arbitrary dimensions, not only on the restricted 2D case. However, to obtain successful searches, a new adjustment for the self-loop weight is necessary. The experiments we made allow to conclude that $l = \frac{2dm}{N}$ is the generalized and optimal value of l for d -dimensional grids with multiple solutions. The fits proposed in previous works are only a specific case where d equals 2. The investigations on d -dimensional grids also made explicit a two-to-one relation between the steps of the LQW and the ones of Grover's algorithm. It turns out an actual amplitude amplification occurs at every two steps, where the first is an intermediary step subject to numerical fluctuations. A fluctuation-tolerant stopping condition is obtained comparing the success probabilities of the current step and the penultimate step, not between subsequent steps.

Future works should mathematically define upper and lower bounds considering the impacts of multiple solutions stated here, which will enable better comparisons between the LQW and other quantum search algorithms. Instead of arranging solutions following a predefined organization, the impacts of solution densities and relative distances should be studied for solutions randomly sampled from some probability distributions. Mathematically or numerically estimated, the number of steps T to the maximum amplitude amplification should be defined *a priori* since it defines the step where the measurement should occur when executed in quantum devices. Based on the generalized l , the number of steps T might also depend on d , L and m . Theoretically, the LQW algorithm will be available to execute in quantum devices, ensuring high success probabilities on d -dimensional grids with multiple solutions. In practice, the LQW implementation will still need to deal with limitations present in the existing quantum hardware. Inspired in [47], future works should implement the LQW algorithm on the available quantum computers. Finally, the LQW algorithm should be applied to solve search problems, like finding weights and biases that train artificial neural networks.

Acknowledgments

This work was supported by the Science and Technology Support Foundation of Pernambuco (FACEPE); the National Council for Scientific and Technological Development (CNPq); and the Coordenação de Aperfeiçoamento de Pessoal de Nível Superior - Brasil (CAPES) - Finance Code 001.

References

- [1] M. A. Nielsen and I. L. Chuang, *Quantum Computation and Quantum Information: 10th Anniversary Edition*. Cambridge: Cambridge University Press, 2010.
- [2] J. Preskill, “Quantum computing and the entanglement frontier,” *arXiv preprint arXiv:1203.5813*, 2012.
- [3] F. Arute, K. Arya, R. Babbush, D. Bacon, J. C. Bardin, R. Barends, R. Biswas, S. Boixo, F. G. S. L. Brandao, D. A. Buell, *et al.*, “Quantum supremacy using a programmable superconducting processor,” *Nature*, vol. 574, no. 7779, pp. 505–510, 2019.
- [4] E. Pednault, J. A. Gunnels, G. Nannicini, L. Horesh, and R. Wisnieff, “Leveraging secondary storage to simulate deep 54-qubit sycamore circuits,” *arXiv preprint arXiv:1910.09534*, 2019.
- [5] J. Preskill, “Quantum computing in the nisq era and beyond,” *Quantum*, vol. 2, p. 79, 2018.
- [6] L. K. Grover, “Quantum mechanics helps in searching for a needle in a haystack,” *Physical review letters*, vol. 79, no. 2, p. 325, 1997.
- [7] P. Benioff, “Space searches with a quantum robot,” in *Quantum Computation and Information (Washington, DC, 2000)* (S. J. Lomonaco Jr. and H. E. Brandt, eds.), vol. 305 of *Contemporary Mathematics*, pp. 1–12, Providence, RI, USA: American Mathematical Society, 2002.
- [8] S. Aaronson and A. Ambainis, “Quantum search of spatial regions,” in *Proceedings of the 44th Annual IEEE Symposium on Foundations of Computer Science (FOCS’03)*, pp. 200–209, IEEE, 2003.
- [9] A. Ambainis, “Quantum walk algorithm for element distinctness,” *SIAM Journal on Computing*, vol. 37, no. 1, pp. 210–239, 2007.
- [10] F. Magniez, M. Santha, and M. Szegedy, “Quantum algorithms for the triangle problem,” *SIAM Journal on Computing*, vol. 37, no. 2, pp. 413–424, 2007.
- [11] E. Farhi, J. Goldstone, and S. Gutmann, “A quantum algorithm for the hamiltonian nand tree,” *arXiv preprint arXiv:quant-ph/0702144*, 2007.
- [12] Y.-G. Yang and Q.-Q. Zhao, “Novel pseudo-random number generator based on quantum random walks,” *Scientific reports*, vol. 6, no. 20362, pp. 1–11, 2016.
- [13] X. Zhan, H. Qin, Z.-h. Bian, J. Li, and P. Xue, “Perfect state transfer and efficient quantum routing: A discrete-time quantum-walk approach,” *Physical Review A*, vol. 90, no. 012331, pp. 1–5, 2014.
- [14] A. M. Childs, “Universal computation by quantum walk,” *Physical Review Letters*, vol. 102, no. 180501, pp. 1–4, 2009.
- [15] N. B. Lovett, S. Cooper, M. Everitt, M. Trevers, and V. Kendon, “Universal quantum computation using the discrete-time quantum walk,” *Physical Review A*, vol. 81, no. 042330, pp. 1–7, 2010.
- [16] Y. Aharonov, L. Davidovich, and N. Zagury, “Quantum random walks,” *Physical Review A*, vol. 48, no. 2, p. 1687, 1993.

- [17] E. Farhi and S. Gutmann, “Quantum computation and decision trees,” *Physical Review A*, vol. 58, no. 2, p. 915, 1998.
- [18] R. Portugal, *Quantum walks and search algorithms*. New York, NY, USA: Springer, 2013.
- [19] A. M. Childs, “On the relationship between continuous- and discrete-time quantum walk,” *Communications in Mathematical Physics*, vol. 294, no. 2, pp. 581–603, 2010.
- [20] A. M. Childs and J. Goldstone, “Spatial search by quantum walk,” *Physical Review A*, vol. 70, no. 2, p. 022314, 2004.
- [21] A. Ambainis, J. Kempe, and A. Rivosh, “Coins make quantum walks faster,” in *Proceedings of the 16th Annual ACM-SIAM Symposium on Discrete Algorithms*, SODA ’05, (USA), pp. 1099–1108, Society for Industrial and Applied Mathematics, 2005.
- [22] A. M. Childs and J. Goldstone, “Spatial search and the dirac equation,” *Physical Review A*, vol. 70, no. 4, p. 042312, 2004.
- [23] D. A. Meyer and T. G. Wong, “Connectivity is a poor indicator of fast quantum search,” *Physical review letters*, vol. 114, no. 11, p. 110503, 2015.
- [24] N. Shenvi, J. Kempe, and K. B. Whaley, “Quantum random-walk search algorithm,” *Physical Review A*, vol. 67, no. 5, p. 052307, 2003.
- [25] T. G. Wong, “Grover search with lackadaisical quantum walks,” *Journal of Physics A: Mathematical and Theoretical*, vol. 48, no. 43, p. 435304, 2015.
- [26] T. G. Wong, “Faster search by lackadaisical quantum walk,” *Quantum Information Processing*, vol. 17, no. 3, p. 68, 2018.
- [27] N. Inui, N. Konno, and E. Segawa, “One-dimensional three-state quantum walk,” *Physical Review E*, vol. 72, no. 056112, pp. 1–7, 2005.
- [28] M. L. Rhodes and T. G. Wong, “Search on vertex-transitive graphs by lackadaisical quantum walk,” *Quantum Information Processing*, vol. 19, no. 9, p. 334, 2020.
- [29] P. Høyer and Z. Yu, “Analysis of lackadaisical quantum walks,” *arXiv preprint arXiv:2002.11234*, 2020.
- [30] A. Saha, R. Majumdar, D. Saha, A. Chakrabarti, and S. Sur-Kolay, “Search of clustered marked states with lackadaisical quantum walks,” *arXiv preprint arXiv:1804.01446*, 2018.
- [31] N. Nahimovs, “Lackadaisical quantum walks with multiple marked vertices,” in *SOFSEM 2019: Theory and Practice of Computer Science* (B. Catania, R. Kráľovič, J. Nawrocki, and G. Pighizzini, eds.), vol. 11376 of *Lecture Notes in Computer Science*, pp. 368–378, Springer, 2019.
- [32] P. R. Giri and V. Korepin, “Lackadaisical quantum walk for spatial search,” *Modern Physics Letters A*, vol. 35, no. 08, p. 2050043, 2020.
- [33] J. H. A. de Carvalho, L. S. de Souza, F. M. de Paula Neto, and T. A. E. Ferreira, “Impacts of multiple solutions on the lackadaisical quantum walk search algorithm,” in *Intelligent Systems* (R. Cerri and R. C. Prati, eds.), vol. 12319 of *Lecture Notes in Computer Science*, pp. 122–135, Springer, 2020.

- [34] N. Nahimovs and R. A. M. Santos, “Lackadaisical quantum walks on 2d grids with multiple marked vertices,” *arXiv preprint arXiv:2104.09955*, 2021.
- [35] L. S. de Souza, J. H. A. de Carvalho, and T. A. E. Ferreira, “Quantum walk to train a classical artificial neural network,” in *8th Brazilian Conference on Intelligent Systems (BRACIS 2019)*, pp. 836–841, IEEE, 2019.
- [36] L. S. de Souza, J. H. A. de Carvalho, and T. A. E. Ferreira, “Classical artificial neural network training using quantum walks as a search procedure,” *IEEE Transactions on Computers*, In press.
- [37] D. McMahon, *Quantum Computing Explained*. New Jersey, USA: John Wiley & Sons, 2007.
- [38] N. D. Mermin, *Quantum Computer Science: An Introduction*. Cambridge: Cambridge University Press, 2007.
- [39] N. S. Yanofsky and M. A. Mannucci, *Quantum Computing for Computer Scientists*. Cambridge: Cambridge University Press, 2008.
- [40] T. G. Wong, “Unstructured search by random and quantum walk,” *arXiv preprint arXiv:2011.14533*, 2020.
- [41] G. Brassard, P. Høyer, M. Mosca, and A. Tapp, “Quantum amplitude amplification and estimation,” in *Quantum Computation and Information (Washington, DC, 2000)* (S. J. Lomonaco Jr. and H. E. Brandt, eds.), vol. 305 of *Contemporary Mathematics*, pp. 53–74, Providence, RI, USA: American Mathematical Society, 2002.
- [42] T. G. Wong, “Coined quantum walks on weighted graphs,” *Journal of Physics A: Mathematical and Theoretical*, vol. 50, no. 47, p. 475301, 2017.
- [43] A. Ambainis, A. Bačkurs, N. Nahimovs, R. Ozols, and A. Rivosh, “Search by quantum walks on two-dimensional grid without amplitude amplification,” in *Theory of Quantum Computation, Communication, and Cryptography* (K. Iwama, Y. Kawano, and M. Muraio, eds.), vol. 7582 of *Lecture Notes in Computer Science*, pp. 87–97, Springer, 2013.
- [44] R. Portugal and T. D. Fernandes, “Quantum search on the two-dimensional lattice using the staggered model with hamiltonians,” *Physical Review A*, vol. 95, no. 4, p. 042341, 2017.
- [45] A. Tulsi, “Faster quantum-walk algorithm for the two-dimensional spatial search,” *Physical Review A*, vol. 78, no. 1, p. 012310, 2008.
- [46] N. Nahimovs and A. Rivosh, “Quantum walks on two-dimensional grids with multiple marked locations,” *International Journal of Foundations of Computer Science*, vol. 29, no. 04, pp. 687–700, 2018.
- [47] F. Acasiete, F. P. Agostini, J. K. Moqadam, and R. Portugal, “Implementation of quantum walks on ibm quantum computers,” *Quantum Information Processing*, vol. 19, no. 12, pp. 1–20, 2020.